

The Crab Nebula and the class of Type II_n-P supernovae caused by sub-energetic electron capture explosions

Nathan Smith*

Steward Observatory, 933 N. Cherry Ave., Tucson, AZ 85721, USA

Accepted 0000, Received 0000, in original form 0000

ABSTRACT

What sort of supernova (SN) gave rise to the Crab Nebula? While there are several indications that the Crab arose from a sub-energetic explosion of an 8–10 M_{\odot} progenitor star, this would appear to conflict with the high luminosity indicated by historical observations. This paper shows that several well-known observed properties of the Crab and SN 1054 are well-matched by a particular breed of Type II_n supernova. The Crab’s properties are best suited to the Type II_n-P subclass (Type II_n spectra with plateau light curves), exemplified by SNe 1994W, 2009kn, and 2011ht. These events probably arise from relatively low-energy (10^{50} erg) explosions with low ^{56}Ni yield that may result from electron-capture SN (ecSN) explosions, but their high visual-wavelength luminosity and Type II_n spectra are dominated by shock interaction with dense circumstellar material (CSM) rather than the usual recombination photosphere. In this interaction, a large fraction of the 10^{50} ergs of total kinetic energy can be converted to visual-wavelength luminosity. After about 120 days, nearly all of the mass outside the neutron star in the CSM and ejecta ends up in a slowly expanding (1000–1500 km s^{-1}) thin dense shell, which is then accelerated and fragmented by the growing pulsar wind nebula (PWN) in the subsequent 1000 yr, producing the complex network of filaments seen today. There is no need to invoke the extended, invisible fast SN envelope hypothesized to reside outside the Crab. As differentiated from a normal SN II-P, SNe II_n-P provide a much better explanation for several observed features of the Crab: (1) No blast wave outside the Crab Nebula filaments, (2) no rapidly expanding SN envelope outside the filaments, (3) a total mass of $\sim 5 M_{\odot}$ swept up in a thin slow shell, (4) a low kinetic energy of the Crab at least an order of magnitude below a normal core-collapse SN, (5) a high peak luminosity (-18 mag) despite the low kinetic energy, (6) chemical abundances consistent with an 8–10 M_{\odot} star, and (7) a low ^{56}Ni yield. A number of other implications are discussed, concerning other Crab-like remnants, the origin of dust in the Crab filaments, diversity in the initial masses of SNe II_n, and the putative association between ecSNe and SN impostors. This model predicts that if/when light echoes from SN 1054 are discovered, they will exhibit a Type II_n spectrum, probably similar to SNe 1994W and 2011ht.

Key words: circumstellar matter — ISM: individual (The Crab Nebula, Messier 1, NGC 1952) — stars: evolution — stars: mass loss — supernovae: individual (SN 1994W, SN 2009kn, SN 2011ht)

1 INTRODUCTION

The Crab pulsar proves that SN 1054 must have marked the final core-collapse supernova (SN) explosion of a massive star — but what exactly was the initial mass of that star, and what were the properties of the explosion that gave rise to the Crab Nebula we see today? Answers to these

basic questions remain highly uncertain, despite decades of intensive and careful observations. A central mystery that has never been resolved is that while SN 1054 was more luminous than a normal Type II SN, the kinetic energy of the Crab Nebula is surprisingly low (about 7×10^{49} erg or less) compared to the canonical 10^{51} ergs of kinetic energy in a typical SN.

The standard explanation for this fundamental puzzle of the Crab, summarized recently by Hester (2008), is that

* Email: nathans@as.arizona.edu

most of the mass and 90% of the kinetic energy of SN 1054 actually reside far *outside* the visual nebula known as the Crab Nebula, in an invisible freely expanding envelope of cold and neutral SN ejecta. This fast envelope, as well as the blast wave one expects at the leading edge of the fast ejecta that collide with the ambient medium, have never been detected to remarkably low upper limits (see below). In this scenario, first articulated by Chevalier (1977), the Crab Nebula that we see is only the thin interface between the expanding synchrotron nebula and the ejected stellar envelope. Some models for the Crab involve an “electron-capture SN” (ecSN) marking the collapse of a degenerate ONeMg core in a star with initial mass 8-10 M_{\odot} (e.g., Nomoto et al. 1982; Nomoto 1987; Miyaji et al. 1980)¹, producing a weaker explosion (typically 10^{50} erg of kinetic energy, instead of 10^{51} for Fe core collapse). These models, however, also predict sub-luminous explosions (Kitaura et al. 2006) due to the under-production of ^{56}Ni compared to Fe core-collapse SNe. Thus, the disagreement between the Crab’s low kinetic energy and the high luminosity of SN 1054 has remained quite puzzling.

This paper proposes a solution to this enduring mystery, enlisting shock interaction with dense circumstellar material (CSM) as seen in many Type IIn SNe. CSM interaction can produce a very luminous SN despite a low total explosion kinetic energy, because a high fraction (typically $\sim 10\text{-}30\%$ or more) of the kinetic energy is converted to radiation. This same model matches many other unusual properties of the Crab, like the slow, thin, filamentary shell that is the direct product of dense CSM interaction, and helps to provide a unifying picture of SN 1054.

The Crab Nebula is one of the most carefully observed objects in the sky, providing a long list of detailed observational constraints for any model.² An abbreviated list of some of the most relevant observed properties of SN 1054 and the Crab Nebula are given below. These are compiled from two comprehensive reviews by Davidson & Fesen (1985) and Hester (2008), except where noted.

1. SN 1054 was certainly a core-collapse event because it produced a neutron star. This could, however, be accomplished either by a standard Fe core collapse, or by an ecSN event. There are a number of reasons to favor the latter.

2. SN 1054 should have been a Type II supernova (had spectra been available), because H emission lines are bright in the Crab filaments. The relative $n(\text{H})/n(\text{He})$ abundance of ~ 2 (Davidson & Fesen 1985) is too high for it to have been a Type IIb event, and certainly not a Type Ib or Ic (Dessart et al. 2012; Haschinger et al. 2012). The only viable known types are then Type II-P, II-L, or IIn.

3. SN 1054 was, however, quite luminous compared to normal SNe II-P and IIb, with a peak absolute visual magnitude of roughly -18 (this is discussed in more detail below

in §2). The average peak luminosity for SNe II-P is around -15.6 , and around -16.7 for SNe IIb (Li et al. 2011).

4. The network of thermally emitting filaments that encloses the synchrotron nebula has an expansion rate suggestive of an origin in SN 1054. While proper motions of the filaments indicate a later ejection date of 1120-1233 A.D. when extrapolated back in time assuming linear expansion (Trimble 1968; Wyckoff & Murray 1977; Bietenholz et al. 1991; Nugent 1998), it is thought that the pulsar wind nebula (PWN) has been pushing outward against the filaments and has accelerated them (e.g., Woltjer 1958), producing a younger apparent age and driving the instabilities that shape the filaments. More recently, Rudi, Fesen, & Yamada (2007) have measured the proper motion of the Crab’s northern “jet”, which is more distant from the pulsar and less likely to be influenced by acceleration from the PWN, and they measure an ejection date of 1055 A.D. ± 24 yr.

5. The total mass in the Crab Nebula’s filaments is difficult to estimate from nebular spectroscopy, but is likely to be around 5 M_{\odot} , although some estimates have been lower (1–2 M_{\odot}). Some additional mass might be hidden in the dense neutral/molecular cores of some filaments that are shielded from UV radiation and not traced by the emission lines used to estimate the mass. Indeed, high resolution images of filaments and blobs do show ionization gradients consistent with self-shielding (e.g., Blair et al. 1997; Sankrit et al. 1998). We adopt $\sim 5 M_{\odot}$ as the total mass in the shell of filaments.

6. The Crab Nebula is expanding slowly, and has extremely low kinetic energy for a SN. Drift scans of the integrated spectrum from the entire nebula show that most of the gas producing the brightest visual-wavelength emission lines is expanding at roughly $\pm 1200 \text{ km s}^{-1}$ (MacAlpine et al. 1989; Fesen et al. 1997; Smith 2003), which we adopt as the representative bulk speed for most of the mass in the filaments. Fainter emission extends to $\pm 2000\text{-}2500 \text{ km s}^{-1}$, but only very low-level emission and a small fraction of the mass extends to that speed. With $\sim 5 M_{\odot}$ expanding at roughly 1200 km s^{-1} , the kinetic energy of the Crab filaments is only 7×10^{49} ergs (and this is more generous than some estimates).

7. No blast wave has ever been detected outside the Crab Nebula in X-ray emission (Mauche & Gorenstein 1989; Predehl & Schmitt 1995; Seward, Gorenstein, & Smith 2006) or radio emission (Frail et al. 1995). A blast wave located outside the Crab at many times the radius of the current filaments is expected in the “standard” model for the Crab Nebula, where a freely expanding, fast, and cold stellar envelope should be colliding with the ambient medium. Attempts to explain the lack of a blast wave require special conditions in the surrounding medium and are generally unsatisfying.

8. No neutral envelope outside the visible filaments with speeds comparable to a normal SN II-P has ever been detected. As above, an extended fast expanding envelope of cold SN ejecta should reside outside the Crab in the standard view. Lundqvist et al. (1986) predicted that because of ionization from the synchrotron emission, this extended envelope would be easily detected in a number of UV absorption lines. Sollerman et al. (2000) presented a weak detection of the C IV $\lambda 1550$ resonance lines in absorption, but did not detect any material moving faster than 2500 km s^{-1} , only tracing about 0.3 M_{\odot} of material at those relatively slow

¹ The range of initial mass for ecSNe varies between studies; some prefer masses near the higher end of this range (see, e.g., Wanajo et al. 2009).

² Here we concentrate on the thermal filamentary shell of the Crab Nebula in order to diagnose properties of SN 1054. We do not discuss the remarkable properties of the synchrotron nebula or the central pulsar, except with respect to their role in shaping and accelerating the filaments long after the SN.

speeds that correspond to the outer parts of the visible filaments. Other upper limits on any fast envelope outside the Crab are quite restrictive (e.g., Fesen et al. 1997), making it unlikely that there is an envelope of several M_{\odot} moving at speeds up to $10,000 \text{ km s}^{-1}$ as one expects if SN 1054 were a normal SN II-P.

9. Analysis of the chemical composition of the Crab Nebula filaments reveals them to be He and C rich, and not as O-enriched as other ccSN remnants (see Davidson & Fesen 1985, and references therein; e.g., Henry & MacAlpine 1982; Pequignot & Dennefeld 1983; Davidson et al. 1982; Fesen & Kirshner 1982; Kirshner 1974; Satterfield et al. 2012). This yield implies a relatively low initial mass for the progenitor star of around $M_{ZAMS} \simeq 8\text{--}10 M_{\odot}$ (some put the initial mass at the higher end of this range; e.g., MacAlpine & Satterfield 2008).

10. The composition of the filaments also indicates relatively low abundances of iron-peak elements, which in turn implies a low yield of ^{56}Ni . This too is consistent with a relatively low-energy ecSN.³

11. The Crab is located about 180 pc from the Galactic plane. Aside from the remote possibility that it could be a runaway from the I Geminorum association (although radial velocities seem to discount this; Minkowski 1970), it does not appear to be associated with any group of OB stars. These facts also seem to point toward a relatively low-mass progenitor star.

12. The Crab filaments formed significant amounts of both dust and molecules, indicating that they went through a phase with very high density and rapid cooling. Dust in the filaments can be inferred based on the absorption it produces, causing some of the filaments to be seen in silhouette against the synchrotron nebula (Fesen & Blair 1990). Far-infrared (IR) thermal emission from dust was recognized early-on (Glaccum et al. 1982; Marsden et al. 1984). The dust mass has been constrained by more recent *Spitzer* and *Herschel* observations (Temim et al. 2006, 2012; Gomez et al. 2012), with a surprisingly large mass of $0.1\text{--}0.2 M_{\odot}$ indicated by the *Herschel* data (Gomez et al. 2012).⁴ IR spectroscopy also reveals the presence of H_2 in the Crab filaments (Graham et al. 1990; Loh, Baldwin, & Ferland 2010; Richardson et al. 2012).

Altogether, the observed parameters listed above present a serious challenge to understanding SN 1054 as a normal Type II explosion (either SN II-P, IIb, or II-L). A large number of unrelated and unlikely circumstances would need to conspire to produce the Crab Nebula from a normal core-collapse SN.

In stark contrast, all of the observational properties listed above are expected and well matched by a particular observed class of SN - namely, the sub-class of Type IIn-P explosions (Type IIn spectra with plateau light curves), dis-

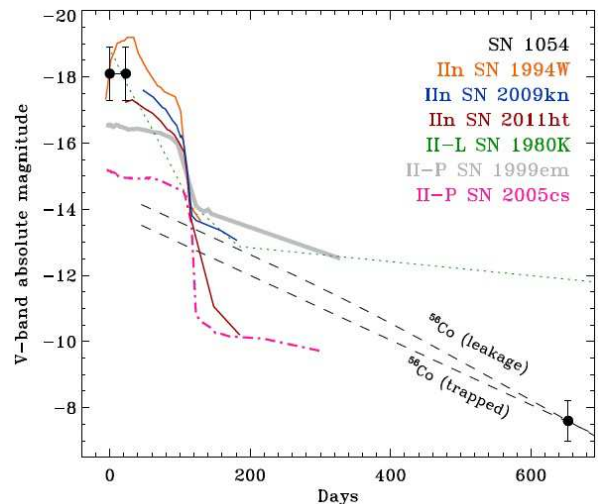


Figure 1. The V-band absolute-magnitude light curves for a number of modern SNe compared to the limited historical information about the visual-wavelength luminosity of SN 1054 (black dots; see text). SN 1994W is from Sollerman et al. (2000), SN 2009kn is from Kankare et al. (2012), and SN 2011ht is from Mauerhan et al. (2013a). SN 1980K is from Buta (1982), with very late-time V-band photometry from Sugerman et al. (2012). SN 1999em is from Leonard et al. (2002), and SN 2005cs is from Pastorello et al. (2009).

cussed recently by Mauerhan et al. (2013a). SNe IIn are fundamentally different from other types of SNe because they are dominated by intense CSM interaction, which sweeps up most of the mass into a cold, dense shell (CDS) that collapses as a result of radiative cooling. It is precisely this radiative cooling that can make SNe IIn very luminous, even with low kinetic energy. For SNe IIn-P, evidence suggests that at least some members of this class are sub-energetic (perhaps even being associated with ecSNe, although this remains unproven), while still being as luminous as normal SNe (or moreso). Details of this comparison are outlined below. We begin with a discussion of the historical light curve and a comparison to modern SNe (§2), followed by a simplified model and sequence of events that accounts for the observed properties (§3). This is followed by a discussion of a number of further implications for the connection between the Crab and SNe IIn-P, including a prediction for the observed spectrum if light echoes are detected from SN 1054, as well as related implications for the interpretation of SNe IIn and SN impostors in general.

2 THE HISTORICAL LIGHT CURVE

The association of the Crab Nebula with the famous “Guest Star” observed by Chinese astrologers, discovered on 1054 July 4, has been recounted many times (Lundmark 1921; Duyvendak 1942; Mayall & Oort 1942; Shklovsky 1968; Minkowski 1971; Clark & Stephenson 1977; Chevalier 1977; Brecher et al. 1983). The weirdness of the Crab compared to other traditional SNe and SN remnants has also been repeated many times, by these same authors and others. Adopting the known extinction of $A_V = 1.6 \text{ mag}$ (Miller

³ Wanajo et al. (2009) point out that the apparent high Ni/Fe ratio inferred for the Crab filaments would also be consistent with the ecSN model.

⁴ The dust mass in the Crab has sparked some recent controversy. While Temim & Dwek (2013) suggest that the large excess far-IR flux detected by *Herschel* does not indicate a large dust mass, P. Owens (2013, private comm.) performed an independent model analysis and finds a large dust mass consistent with the analysis by Gomez et al. (2012).

1973) and a distance of ~ 2 kpc (Trimble 1973; or 1500–2200 pc as given by Davidson & Fesen 1985), one can translate the historical accounts of Chinese astrologers to approximate absolute magnitudes (roughly V -band). There are essentially two facts that we gain from the historical reports:

- *SN 1054 was visible during daytime for a total of 23 days.* Following Shklovsky (1968), this implies $m_{vis} \simeq m_V \simeq -5$ mag, and therefore an absolute visual magnitude of about -18.1 or brighter during those 23 days. It is not known how day 23 compares to the time after explosion, because the discovery on July 4 may have been the date when SN 1054 first appeared in the early morning after being behind the Sun (it is a fall and winter object). Thus, the peak absolute magnitude is not firmly established (i.e., it is at least as luminous as -18 mag during that time, but could have been more luminous at earlier times). The time when SN 1054 was seen during the day is marked by the first two black dots in Figure 1, adopting an uncertainty of ± 0.8 mag (although the first point should perhaps be regarded as a lower limit to the initial luminosity).

- *SN 1054 faded thereafter, and remained visible at night to the unaided eye until 653 days after discovery.* The rate of fading is not known, but we can conclude that by day 653 the SN had faded to a luminosity of about $M_V = -7.6$ mag. This is indicated by the last black dot on Figure 1, adopting a somewhat smaller uncertainty of ± 0.6 mag).

What do these two facts tell us about the type of SN that made the Crab? Before considering that question, let’s remember that we can rule out SNe Ib and Ic, and probably also IIb, because of the presence of substantial amounts of H in the Crab filaments. Considering only SNe of Type II, then, Figure 1 does provide some useful constraints.

Figure 1 allows us to rule out normal SNe II-P like SN 1999em and fainter SNe II-P like SN 2005cs because they never achieve such a high peak luminosity. This is quite useful information, because one class of SNe that is consistent with *some* available information about the Crab is the group of low-luminosity SNe II-P, which could be caused by low-energy ecSNe that would agree with the kinetic energy and abundances of the Crab, and its implied low-mass progenitor star. However, the high peak luminosity of -18 mag clearly rules these out (at least without some mechanism to make them more luminous).

There are some relatively luminous SNe II-P (Li et al. 2011; Elias-Rosa et al. 2009; Arcavi et al. 2012) that approach the peak luminosity of SN 1054, but these are thought to be luminous because of an energetic explosion that synthesizes a relatively large mass of ^{56}Ni . A large mass of ^{56}Ni would produce a luminous radioactive decay tail that would be too bright (in fact, according to Figure 1 even SN 1999em would be too luminous at late times). Moreover, a large mass of ^{56}Ni is in conflict with the observed abundances of the Crab, which are deficient in Fe-group elements (see above). This means that attributing the late-time faintness to dust formation alone does not solve the problem. Some SNe II-L do have brighter peak luminosities around -17 to -18 mag, but they tend to fade slowly and are more luminous at late times than SN 1054. The canonical SN II-L 1980K is shown in Figure 1 for comparison. Normal SNe II in like SN 1998S have light curves very similar to SNe II-L, and do achieve peak luminosities like SN 1054. However, these

also tend to fade more slowly, and remain luminous at late times due to ongoing CSM interaction.

Finally, there is an observed class of SNe that does seem to agree well with the historical light curve of SN 1054, and that is the class of SNe II-n-P (Mauerhan et al. 2013a). The V -band light curves of SN 1994W, SN 2009kn, and SN 2011ht are shown in Figure 1. Like traditional SNe II-n, they can achieve relatively high peak luminosities in agreement with SN 1054, and indeed they often fade significantly during their “plateau”. What is unique about these SNe is that, unlike other SNe II-n, their luminosity plummets after ~ 120 days so that they do not maintain the high level of CSM interaction luminosity at late times seen in most SNe II-n. It has been suggested (Mauerhan et al. 2013a; Sollerman et al. 2001) that this rapid fading may indicate unusually low yields of ^{56}Ni , or efficient dust formation (or both). This drop should also be accompanied by a drop in CSM interaction, although the reason why all these SNe would do this at ~ 120 days is not obvious (Mauerhan et al. 2013a). The drop from the end of the plateau is more extreme in some SNe II-n-P as compared to others. The most extreme drop after the plateau is for the case of SN 2011ht, but in this case we know that the colors became very red, whereas the bolometric luminosity did not drop quite so much (Mauerhan et al. 2013a). Once again, dust formation may be influential, whereas SN 2009kn may have formed less dust and consequently had bluer colors on its decay tail. The rapid drop after the plateau probably correlates with low ^{56}Ni mass, as in low-luminosity SNe II-P.

For comparison, Figure 1 also includes representative fading rates due to radioactive decay at late times (black dashed lines), matched to the one late-time luminosity constraint for SN 1054. Two cases are shown: (1) all the γ -ray luminosity is trapped by the ejecta and reprocessed into visual light, which would indicate a mass of synthesized ^{56}Ni of about $0.009 M_{\odot}$, and (2) some leakage of the γ -rays produced by radioactive decay (where the γ -ray optical depth evolves as $\tau \propto t^{-2}$, following Sollerman et al. 2001), yielding a somewhat larger mass of $M(^{56}\text{Ni}) = 0.016 M_{\odot}$. Both are significantly less than the ^{56}Ni mass expected from a normal 10^{51} erg SN event. As we discuss below, however (and as mentioned by Sollerman et al. 2001), CSM interaction may also make a contribution to the late time luminosity, potentially lowering the ^{56}Ni mass further.

How does the apparent uniqueness of the Crab compare to the frequency of various SN subtypes? The Crab Nebula is the only one of its kind among the handful of known Galactic SN remnants that are connected to historically observed events, provoking many commentaries about how unique or bizarre it is. Considering the statistics, we note that SNe of Type II-n make up only 8-9% of all core-collapse SNe in a volume-limited sample (Smith et al. 2011a), and an even lower fraction of all SNe if Type Ia events are included (Li et al. 2011). Moreover, the SN II-n-P subclass represents only a subset of all SNe II-n. The apparently unique character of the Crab among young nearby SN remnants in the Galaxy is therefore not so surprising if SN 1054 was a Type II-n-P event, but it is very difficult to reconcile with the idea that SN 1054 was a normal SN II-P in which most of the mass and kinetic energy have gone undetected at the present time. This is discussed further in §4.2 and §4.5.

3 CSM INTERACTION LUMINOSITY

The observational case outlined in the previous section makes a compelling argument that SN 1054 shared properties in common with SNe IIn, and the sub-class of SNe IIn-P in particular. We must discuss whether this makes sense physically as well as observationally. This section outlines a very simple baseline model of CSM interaction that can account for both the luminosity of the events (SN 1054 and the class of SNe IIn-P) and the resulting mass, kinematics, and structure of the Crab Nebula.

3.1 A Simple Model for SNe IIn-P

Let’s begin with some order-of-magnitude estimates. For SNe IIn-P and for SN 1054, we wish for the shock interaction between the explosion ejecta and the dense CSM to achieve a luminosity of order -18 mag or $\sim 10^9 L_\odot$ for the first few months.

In this scenario, dense CSM decelerates the shock, and the resulting high densities in the post-shock region allow the shock to become radiative (i.e. the shock becomes momentum conserving instead of energy conserving, as in all SNe IIn). With high densities and optical depths in H-rich gas, thermal energy is radiated away primarily as visual-wavelength continuum emission. This loss of energy removes pressure support behind the forward shock, leading to a very thin, dense, and rapidly cooling shell at the contact discontinuity (usually referred to as the “cold dense shell”, or CDS; see Chugai et al. 2004; Chugai & Danziger 1994). This CDS is pushed by ejecta entering the reverse shock, and it is slowed and mass-loaded by the CSM, into which it expands at a speed V_{CDS} . In this scenario, the maximum emergent continuum luminosity from CSM interaction is given by

$$L_{CSM} = \frac{1}{2} \dot{M} \frac{V_{CDS}^3}{V_W} = \frac{1}{2} w V_{CDS}^3 \quad (1)$$

where V_{CDS} is the outward expansion speed of the CDS, V_W is the speed of the pre-shock wind, \dot{M} is the mass-loss rate of the wind, and $w = \dot{M}/V_W$ is the so-called wind density parameter (see Chugai et al. 2004; Chugai & Danziger 1994; Smith et al. 2010).⁵

For a radiated luminosity of $10^9 L_\odot$ and for an assumed expansion speed of the CDS of around 1100 km s^{-1} (recall that the present speed of $\sim 1200 \text{ km s}^{-1}$ in the Crab filaments is the result of later acceleration by the PWN), we require a CSM density of order $w \approx 6 \times 10^{18} \text{ g cm}^{-3}$. The total mass in the CSM would be $\sim 3 M_\odot R_{15}^{-1}$, where R_{15} is the outer radius of the CSM shell in units of 10^{15} cm .

Note that according to Equation (1) we could also achieve a very high CSM interaction luminosity with less dense CSM but with a faster shock speed, due to the v^3 dependence. For example, we could also reach $L \simeq 10^9 L_\odot$ with $V_{shock} = 10^4 \text{ km s}^{-1}$ and $w = 8 \times 10^{15} \text{ g cm}^{-3}$. This is, however, infeasible for the Crab because CSM interaction must also conserve momentum, and in this scenario with a

faster shock, the lower masses of the CSM and SN ejecta (which together would need to be less than $1 M_\odot$) are ruled out by the observed mass and speed of the Crab filaments. A low CDS shock speed and a low energy are needed to match the observed constraints of the Crab, whereas we do not have independent constraints on the CDS mass in the case of extragalactic SNe IIn-P.

The observed visual CSM-interaction luminosity should be close to the total bolometric luminosity during the bright “plateau” phase of the event (i.e. a small bolometric correction), judging from the apparent temperatures of ~ 6000 – 7000 K typically seen in the continua of virtually all SNe IIn. This may not be strictly true if the apparent temperature changes with time as the shock slows down. In that case the estimated mass-loss rate or the ejecta speed might need to be increased slightly, which doesn’t significantly change the nature of the event discussed here. To be sure, CSM interaction does afford some flexibility in model parameters.

One can also adjust the geometry so that the interaction has a different strength at various latitudes. Small differences of this sort may account for the variation from one SN IIn-P to the next, and there does appear to be some departure from spherical geometry in the CSM interaction that yielded the Crab Nebula (see below). The purpose here is to be illustrative rather than exact, in order to demonstrate that CSM interaction can naturally fix the long-standing puzzle of the high peak luminosity of SN 1054 being apparently at odds with the low kinetic energy of the Crab.

3.2 Origin of the Dense CSM

Equation (1) suggests that SN 1054 requires a wind density parameter of $w \approx 6 \times 10^{18} \text{ g cm}^{-3}$, which implies a total CSM mass of about $3 M_\odot$ within 10^{15} cm of the progenitor. Since the progenitor wind speed (V_W) is not known, there is uncertainty about the mass-loss rate, the nature of the pre-SN mass loss, and the physical state of the progenitor star.

Dense and massive CSM could arise from a sudden explosive or eruptive pre-SN ejection event ($\sim 10^{49} \text{ erg}$) occurring a few years before the SN, as has been hypothesized for more luminous SNe IIn such as SN 2006gy (Smith & McCray 2007, Smith et al. 2010a), for SN 1994W (Chugai et al. 2004), and a number of other SNe IIn. There is now observed precedent for this type of event associated with SNe IIn from the documented series of pre-SN luminous blue variable (LBV)-like events that were actually detected before the SN in the case of SN 2009ip (see Mauerhan et al. 2013b and references therein). There was also a brief pre-SN outburst observed 2 yr before SN 2006jc (Pastorello et al. 2007), but that event was a Type Ibn instead of a Type IIn. The fact that this type of precursor burst has been detected in both SNe IIn and Ibn is very interesting with regard to the Crab, however, given the high He abundance in the Crab filaments. There is also some theoretical motivation for this type of pre-SN eruption in stars of 8 – $10 M_\odot$ due to Ne flashes in the degenerate core (Chugai et al. 2004; Arnett 1974; Hillebrandt 1982; Weaver & Woosley 1979). Alternatively, some evolution models for super-AGB stars in this mass range become unstable due to strong He flashes that cause the star’s interior to exceed the classical Eddington limit, possibly causing hydrodynamic ejection (Wood &

⁵ Note that this scenario where radiation escapes efficiently is somewhat different from a more extreme case where the radiation diffusion time is comparable to the expansion timescale, changing the shape of the light curve (Smith & McCray 2007; Chevalier & Irwin 2011; Falk & Arnett 1977).

Faulkner 1986; Lau et al. 2012). Although Lau et al. (2012) also note that the ensuing mass loss in this scenario could lead the star to avoid the ecSN fate.

A second possibility is that the dense CSM would come from a steady, short-duration wind. For a fiducial pre-shock CSM speed of 10 km s^{-1} , this would translate to a progenitor mass-loss rate of $\sim 10^{-1} M_{\odot} \text{ yr}^{-1}$ blowing for ~ 30 yr before the SN. This timescale would achieve the desired outer CSM radius of $\sim 10^{15} \text{ cm}$. Such a high wind mass-loss rate from a relatively low-mass star seems difficult to achieve, however, since stars of this mass are not expected to undergo prolonged super-Eddington phases.

One last alternative has properties that fit well with some theoretical predictions for stars in the right range of initial masses. The CSM mass required to power SN 1054 and SNe IIn-P through interaction might come from the dense wind of a super-AGB star with $\dot{M} \simeq 10^{-4} M_{\odot} \text{ yr}^{-1}$, blowing for a few 10^4 yr to achieve the desired total CSM mass of $\sim 3 M_{\odot}$. A few 10^4 yr duration and $\dot{M} \simeq 10^{-4} M_{\odot} \text{ yr}^{-1}$ is expected for the thermal-pulsing asymptotic giant branch (TP-AGB) phase associated with super-AGB stars of initial mass 8-10 M_{\odot} . In fact, precisely this scenario is found in some stellar evolution models for the super-AGB progenitors of ecSNe (see, e.g., Figure 15 of Poelarends et al. 2008). The difficulty with this scenario is that the massive CSM must be confined to within a few 10^{15} cm in order to provide a high-enough density to power the early light curve and the right duration of the plateau, whereas a super-AGB wind in free expansion blowing for a few 10^4 yr could extend to $\sim 0.1 \text{ pc}$.

Thus, the dense CSM required would seem to be either a short-duration enhanced mass loss phase before core-collapse, or a longer-duration wind that is somehow confined within a smaller volume (either by external pressure of a previous hot-wind phase or gravity of a companion star, for example). These are unsolved issues, but it is nevertheless true that the observed light curves of SNe IIn-P require very dense CSM with this very compact radial extent. Below we explore models using CSM environments with density that falls off as R^{-2} (as in a wind) and a CSM with constant density (as in a pressure-confined wind or perhaps an ejected shell). This distinction turns out to cause only minor differences in the mass and energy requirements.

3.3 The Light Curve from CSM Interaction

Equation (1) provides a very rough estimate of the CSM density needed to power the peak luminosity with CSM interaction. To compute a simple model light curve and to derive better estimates of the energy and mass involved, however, we must account for the fact that the speed of the CDS and the speed of SN ejecta crashing into the CDS will change with time. We adopt a simple spherically symmetric model where relatively low-energy ($\sim 10^{50} \text{ erg}$) ejecta collide with dense CSM. At each time-step in the ensuing collision, the CDS conserves momentum contributed by the SN ejecta and CSM. The deceleration of the faster SN ejecta upon joining the CDS leads to a drop in the kinetic energy, and the difference between the initial and final kinetic energy at each time step provides the emergent luminosity at that time, from which the light curve is calculated. (Although this light curve represents the maximum possible bolometric

luminosity, we assume that this is close to the visual luminosity since the CDS is optically thick and its peak flux is in optical light. This should be true during the bright plateau phase, but may become a worse approximation at late times as the optical depth drops.) This is essentially the same type of model used to calculate the CSM interaction luminosity of the $\sim 10^{50} \text{ erg}$ Great Eruption of η Carinae (Smith 2013), except that the CSM and ejecta speeds and mass were different in that model, which led to a fainter luminosity with a longer duration.

We consider two cases for the CSM, with a model that has $\rho \propto R^{-2}$, as would be appropriate for a steady short-duration wind, and with a model that adopts a constant-density CSM envelope (as used by Chugai et al. 2004 in the case of SN 1994W), which would be more appropriate for a pressure-confined CSM or perhaps for an eruptive event. The resulting light curves for the two cases are shown in the top panels of Figures 2 and 3, respectively. The bottom panels of both figures plot the time evolution of the radius and speed of the CDS corresponding to each model.

The main difference between the two model light curves is in the shape of the plateau. Since more CSM mass is located at larger radii in the constant density CSM model, this light curve has a flatter plateau and it takes a longer time to rise to peak luminosity. For this reason, the light curve plotted in Figure 3 has been shifted in time by -40 days due to a larger delay between the time of explosion and the time of discovery by visual observers. Although this is a crude model, the resulting light curves are very similar to light curves of SN/CSM interaction produced using more detailed 1-D and 2-D hydrodynamic simulations (e.g., van Marle et al. 2010; Woosley et al. 2007).

The drop in luminosity at the end of the plateau arises because the expanding CDS reaches the outer edge of the dense CSM, at which time CSM interaction ends. The time at which this occurs is set by the choice of the outer radius of the CSM, which is chosen to be 120 days as seen in SNe IIn-P, and the speed at which the CDS moves through the CSM. This is easily adjusted and is not a critical part of the model for the Crab, however, since there are not (yet) any observational constraints on the duration (or existence) of a plateau in SN 1054. The steep drop in the model plateau is somewhat artificial, dictated by the assumed instantaneous drop in density at the outer boundary of the CSM in the simple model; in reality, it is likely that this transition would be smoother, as observed in SNe IIn-P.

After the plateau ends and the luminosity drops at ~ 120 days, there is a tail of declining luminosity. There are two likely contributions to this late-time luminosity. First, even though the CDS is no longer sweeping into dense CSM ahead of the shock, there would still be some luminosity contributed by ongoing shock interaction as the remaining inner SN ejecta catch up to the dense and slowly expanding CDS. This shock luminosity drops with time because of the shrinking difference between CDS speed (now coasting at constant speed) and the speed of freely expanding SN ejecta (slower ejecta take longer to catch up to the CDS). The strength of this ongoing shock interaction is set by the final mass and speed of the CDS at the end of the plateau. The second expected contribution to the late-time luminosity is from radioactive decay, which is observed to be low in SNe IIn-P and should be low in SN 1054 due to the low abun-

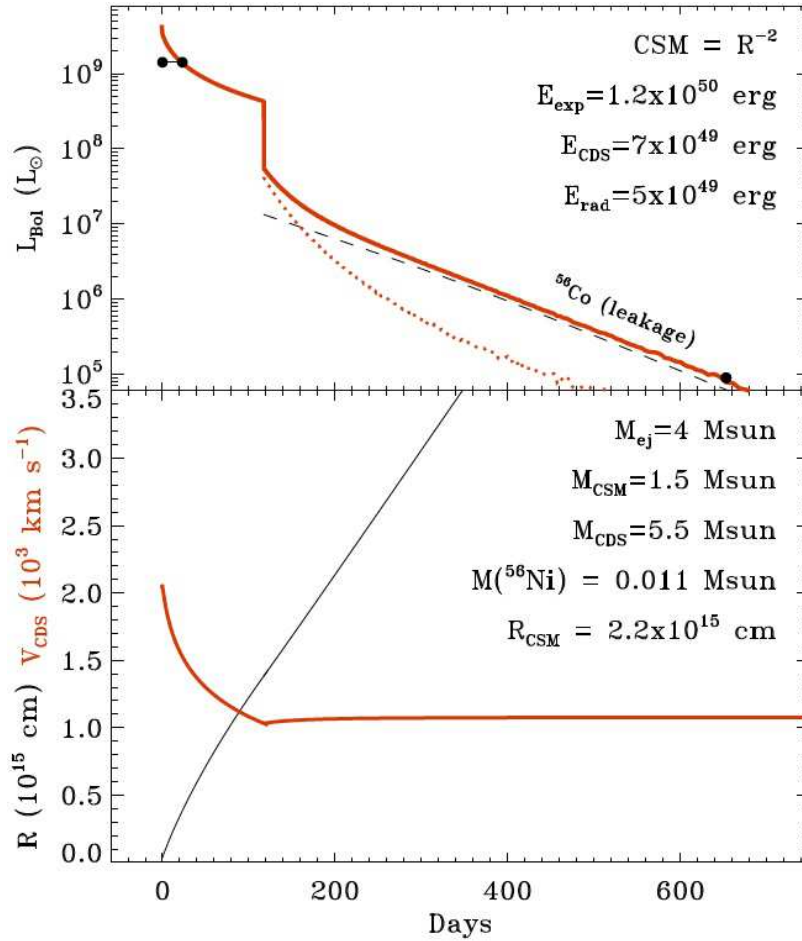


Figure 2. Plots of a CSM-interaction model adopting a CSM with an R^{-2} density law. The top panel shows the radiated bolometric luminosity (orange), which is expected to be similar to the visual luminosity for a SN IIn, compared to the observational constraints for SN 1054 (black dots). The solid orange line shows the total CSM-interaction luminosity added to the radioactive decay luminosity (with some leakage, same as in Figure 1), the dashed black line is the radioactive decay luminosity alone, and the dotted orange line is the late-time luminosity from CSM interaction alone, excluding radioactive decay. The bottom panel shows corresponding plots of the radius (black) and velocity (orange) of the CDS with time. Assumed (explosion energy, ejecta mass, CSM mass, final mass swept into the CDS) and derived (final kinetic energy of the CDS, total radiated energy, synthesized ^{56}Ni mass, outer radius of the CSM) physical parameters in the model are listed along the right side of the figure.

dance of Fe-group elements in the Crab. Even if we allow for some γ -ray leakage (see above), the implied masses of ^{56}Ni synthesized in the explosion are of order $0.01 M_{\odot}$. The solid orange curves at late times show the sum of the radioactive decay and shock luminosity, while each individual contribution is shown separately with dotted and dashed curves. This late-time luminosity does not include any contribution from luminosity that might be associated with early spin-down of the young neutron star; core-collapse simulations (e.g., Ott et al. 2006) yield shorter periods than one expects from extrapolating the present-day spin period of 33 ms for the Crab. Some loss of rotational energy is probably required, although the mechanism and possible luminosity associated with this are uncertain.

Both models in Figures 2 and 3 with somewhat different CSM density distributions provide an adequate account of the peak luminosity and late time luminosity of SN 1054, and moreover, the final properties of the coasting CDS match the mass, speed, and kinetic energy of the Crab filaments.

The model with density falling as R^{-2} would seem to do a better job of accounting for the fact that SN 1054 was only at its peak luminosity for a relatively short time of 23 days, whereas the longer plateau that arises from constant density would seem to match some of the SN IIn-P light curves a bit better. The distinction between these two is subtle, and proper radiative transfer may provide better constraints on the emergent temperature and bolometric correction (these plots are just the total bolometric radiated luminosity). The true density distribution may be between the two cases illustrated here, and it may of course be non-spherical, but the order of magnitude in the CSM density and mass must be roughly correct.

Although the model used here is quite simplified, it adequately demonstrates that a relatively low-energy 10^{50} erg explosion that would be expected from an ecSN can produce both the high peak luminosity and low late-time luminosity of SNe IIn-P and SN 1054. It also securely demonstrates that CSM interaction allows the light curve to be reconciled

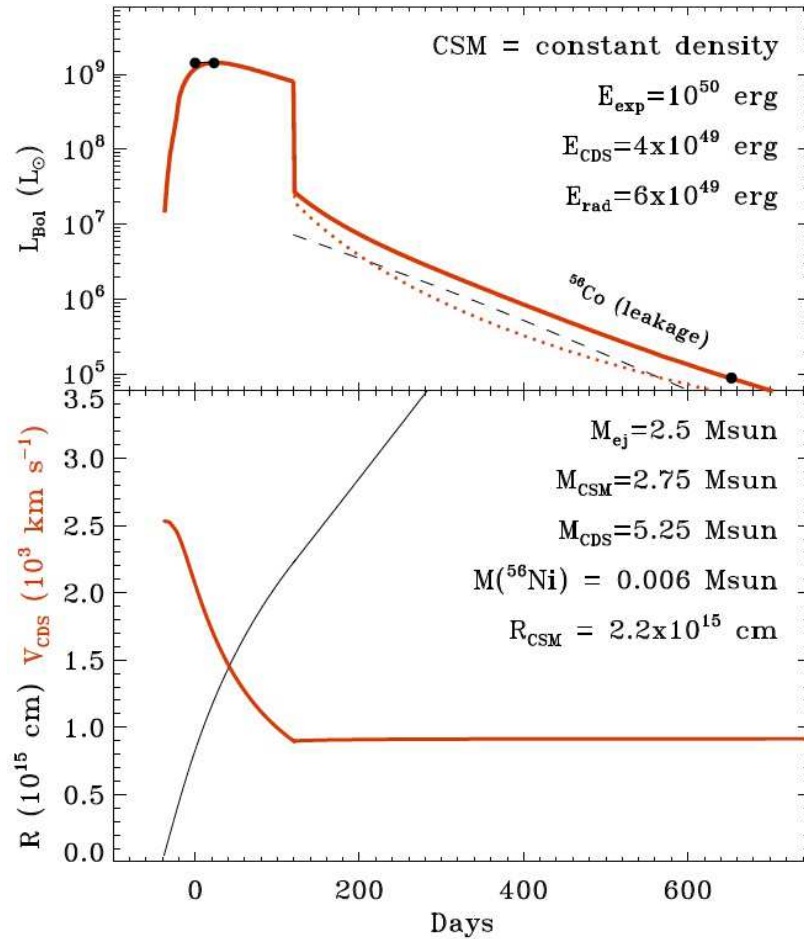


Figure 3. Same as Figure 2, but with a CSM that has constant density. One difference is that the model has been shifted by -40 days due to the fact that the constant density CSM model takes a longer time for the light curve to rise to peak, and would likely be discovered later, relative to the R^{-2} CSM model in Figure 2.

with the present-day observed properties of the Crab filaments. Since the forward shock has been decelerated by the dense CSM, no additional mass or SN energy needs to be hidden outside the observed Crab filaments in this model.

3.4 A Sequence of Events for the Crab

How did the complex structure of the Crab Nebula we see today – including its spectacularly complex web of dense filaments – arise as a result of the CSM interaction model described above? Figure 4 illustrates a possible sequence of events that would lead to the basic structures seen in the scenario where SN 1054 was a Type II_n-P explosion.

In this model, the progenitor star must have been a relatively low-mass ($8-10 M_{\odot}$) super-AGB star surrounded by a dense shell of CSM within about $1-2 \times 10^{15}$ cm of the central star (Figure 4a). To account for some specific structures seen in the Crab (see below), this initial configuration includes a density enhancement near the equatorial plane of the progenitor star, with this “disk” seen roughly edge-on and with an east/west orientation. This disk is not needed to explain the light curve.

Immediately after core collapse, the remaining stellar envelope that had not already been shed in the pre-SN mass

loss expands outward into the dense CSM (Figure 4b). This collision, which lasts of order 120 days, produces the peak luminosity phase of SN 1054 as ejecta kinetic energy is converted to visual-wavelength radiation. In this process, the slow CSM is accelerated and the fast SN ejecta are decelerated; both pile up in the very thin cold dense shell (CDS) that expands outward at about 1000 km s^{-1} . The shell is thin because it collapses to a dense layer as radiation cools the gas and removes pressure support from the post-shock region.

This intense phase of interaction continues until the shock reaches the outer boundary of the dense CSM (Figure 4c). After that time, the luminosity would plummet (at a decline rate dictated by the steepness in the density drop, which is not constrained by available observations). By this time, about $5 M_{\odot}$ has piled up in the slowly expanding CDS, which would coast at a speed of $\sim 1100 \text{ km s}^{-1}$ after this time. The thin shell is composed entirely of SN ejecta and CSM ejected before the explosion, and its chemical abundances reflect the He-rich abundances in the star’s envelope in the final phases of its evolution. Some of the slower ejecta continue to crash into the reverse shock and heat the CDS, but this ongoing shock interaction is far less intense than during the plateau phase.

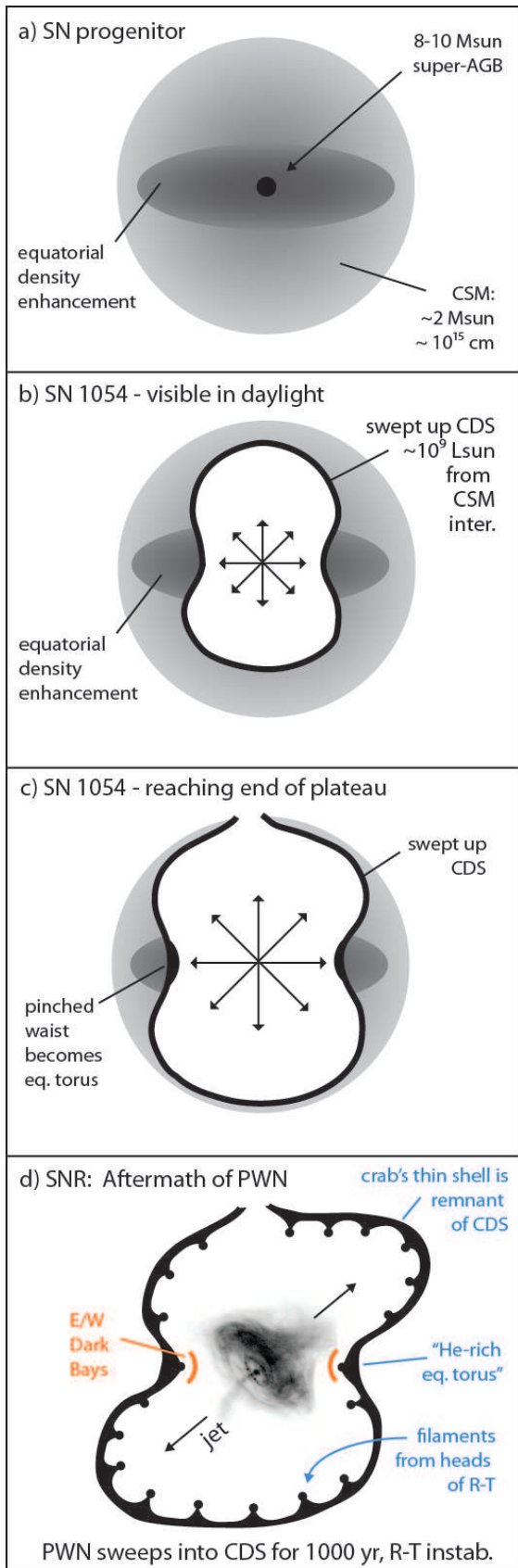


Figure 4. Sketch of a possible sequence of events. See text §3.4.

After this, the CDS would simply continue to coast, were it not for the fact that SN 1054 also gave birth to a pulsar than energizes a PWN. For the next ~ 1000 yr up until modern times, the expansion of the PWN must contend with a massive, slow-moving shell that is in its path of expansion. It is this last phase of the PWN interacting with the thin shell that produces much of the complex structure seen in the Crab (Figure 4d). It is known that the expansion of the PWN has pushed and accelerated the Crab filaments, since their measured proper motions would seem to indicate an origin 70-80 yr after 1054 A.D. (Trimble 1968; Wyckoff & Murray 1977; Bietenholtz et al. 1991; Nugent 1998). In this scenario, where a thin shell is accelerated outward by an underlying fluid, the thin shell will be subject to severe Rayleigh-Taylor (RT) instabilities, and the thin shell will fragment into a network of dense filaments. As the PWN tries to push through the spaces between these filaments, it could give rise to the bubble-like morphology in the outer “[O III] skin” seen in deep exposures of the Crab (Fesen & Gull 1986). In some locations, the PWN may push through the shell, perhaps leading to breakout structures akin to the “chimney” or “jet” on the northern perimeter of the Crab (Fesen & Gull 1982; Cox et al. 1991), although this is speculative. Hydrodynamic simulations of the PWN pushing into a massive CDS that results from a Type II_n explosion might be illuminating.

The overall non-spherical geometry can also be accounted for in this interaction. Fesen, Martin, & Shull (1992) have provided a detailed discussion of the prominent indentations in the Crab synchrotron nebula known as the east and west “bays”. These features mark a location where the continuum synchrotron emission is absent, apparently because the expansion of the PWN has been thwarted there. Fesen et al. (1992) suggested that this may be the result of an equatorial disk-like distribution of dense CSM around the progenitor star, that pinched the waist of the expanding remnant, and they also pointed out a connection to the belt of He-rich filaments that share the same basic orientation as the E and W bays but at larger radii (see also Uomoto & MacAlpine 1987; MacAlpine et al. 1989; Lawrence et al. 1995). This is quite easily accommodated in the CSM interaction scenario for the Crab if the pre-SN CSM shell had an equatorial density enhancement, with an equator/pole density contrast of order 2. The common orientation of the bays and the He-rich torus are harder to accommodate in the “standard” view of the Crab, where the observed Crab filaments are solely the result of the PWN expanding into the freely expanding SN ejecta (Hester 2008); i.e. no interaction with the CSM has occurred here because the hypothetical forward shock is located far outside the Crab. In this scenario, the SE/NW elongation axis of the Crab would arise because of a stronger push along this axis from the Crab’s synchrotron jet, known to share this orientation (see Fig. 4d).

4 PREDICTIONS AND IMPLICATIONS

4.1 Light Echoes

The bright peak luminosity phase of a SN event sends a pulse of light into its surroundings, which can be seen after a time

delay if the light scatters off nearby dust clouds. Such “light echoes” were seen in the surroundings of SN 1987A (e.g., Crotts et al. 1989; Sugerman et al. 2005), and light echoes have now been detected in images and studied spectroscopically for several historical SNe (Rest et al. 2005, 2008a; Krause et al. 2008b). Light echoes from Cas A determined that it was a Type IIb SN (Rest et al. 2008b, 2011a, 2011b; Krause et al. 2008a), even though it is unclear if its 17th century SN event was ever observed directly. Light echoes have even been detected from the 19th century Great Eruption of η Carinae (Rest et al. 2012). Because η Carinae’s peak luminosity was much lower than a SN, and because its peak apparent magnitude was much fainter than SN 1054, there may yet be hope that continuing efforts will be able to identify light echoes from SN 1054, despite its old age of ~ 1000 yr and low-density environment. This is a difficult task, but in the event that light echoes of SN 1054 can be identified, they offer the opportunity to directly test the model proposed here. This prediction may provide a rather definitive and useful test.

The “standard” picture for the Crab (Hester 2008) places most of the mass and most of the kinetic energy outside the filaments in a fast, freely expanding envelope. At the present time this envelope is transparent and invisible, and produces no detectable shock as it encounters the surrounding medium. During the peak luminosity phase of SN 1054, however, the fast envelope would dominate the observed spectrum with a recombination photosphere moving back through the rapidly expanding ejecta. In this scenario, the spectrum should show only broad (5000-10000 km s⁻¹) emission lines with similarly broad P Cygni profiles that should appear to be typical of normal SNe II-P.

On the other hand, if the CSM interaction model advocated here is correct, the SN ejecta are quickly decelerated by dense CSM, giving rise to a high luminosity generated by the collision. In the CSM interaction scenario, the peak luminosity spectrum should exhibit narrow lines typical of SNe II_n. This might include some broad wings or intermediate-width components that are typically seen in SNe II_n, of course, but the strongest emission in the cores of the lines should be narrow (less than about 1000-1500 km s⁻¹, matching the speed of the CDS). In particular, the spectra of light echoes from SN 1054 should closely resemble the spectra of the subclass of SNe II_n-P, like SNe 1994W, 2009kn, and 2011ht (Chugai et al. 2004; Kankare et al. 2012; Mauerhan et al. 2013a), for which high-quality spectra exist.

In addition, the brightness evolution of light echoes can provide information about the historical light curve, usually providing better time sampling than the original historical observations. This would be very useful, given the sparse observations of SN 1054. The light curves derived from images of light echoes of SN 1054 may show a plateau that drops after 120 days if SN 1054 really is a SN II_n-P, or a smoother decline if it is a more traditional SN II_n (or some other type of SN). However, the plateau is less important than the presence of a Type II_n spectrum in order to confirm the essence of the suggested model, since a normal Type II-P will also have a plateau.

4.2 A Closer Look at Other Crab-like Remnants

The scenario suggested here, wherein the Crab is the result of a Type II_n SN, may be relevant to the larger class of Crab-like SNRs and PWNe in general. The Crab is the archetype for a class of filled-center supernova remnants (SNRs) known as PWNe (Gaensler & Slane 2006), also sometimes referred to as filled-center remnants or “plerions” (e.g., Gaensler 2001; Reynolds 1985). The filled center refers, of course, to the bright pulsar-powered synchrotron nebula in the interior of the Crab and its siblings. The class includes other famous objects like the Crab’s twin SNR 0540-69.3 with its young 50 ms pulsar (e.g., Morse et al. 2006; Seward et al. 1984), and 3C58 (Weiler & Seielstad 1971; Weiler 1983) that is possibly associated with SN 1181 (Clark & Stephenson 1977).

It is natural to ask if the physics of a Type II_n explosion can yield favorable conditions to enhance the observability or physical properties of PWNe, or to change their physical properties in a systematic way. Namely, SNe II_n are distinct from other types of SNe in that the end product of the explosion is a slow, thin, and very massive (5-10 M_{\odot} or more) dense shell of swept-up CSM and ejecta. If a pulsar is born in the core-collapse event associated with a SN II_n, its PWN nebula must push outward against this slow and massive shell. Essentially, it may be possible that the CDS in a SN II_n acts as a “cage” to confine the PWN, restricting its expansion and thereby increasing the energy density inside the volume of the PWN. This may make the PWN appear brighter than it otherwise would be.⁶ A pulsar born in a normal SN II-P would only need to push outward against the slowest inner ejecta of the SN, which constitute a much smaller fraction of the total mass of the progenitor star, and may not as easily confine the PWN.

4.3 The Invisible Fast Envelope and Forward Shock of the Crab

If the Crab Nebula is the end product of a Type II_n SN explosion, as described above, then there is no need to invoke the existence of a hypothetical extended, rapidly expanding SN envelope outside the Crab that retains most of the mass and energy of the exploded star (Hester 2008). In a model where a Type II_n event powers the high luminosity of SN 1054 despite the low explosion energy, the outer edge of the Crab’s shell of thermal filaments is the remnant of the CDS. The lack of any observational evidence for the putative fast envelope and the lack of any observed signature of a blast wave far outside the Crab are both, therefore, expected if SN 1054 was a Type II_n event. This model predicts that continued efforts to measure a massive outer fast envelope will only produce deeper upper limits. There is a possibility that there could be a remaining exterior blast wave if the forward shock accelerated through a steep density gradient after exiting a dense CSM shell (see Smith 2013), but this would involve very little mass and kinetic energy, and has probably cooled significantly in the past 1000 yr since explosion. We do not expect to see an extended, fast, cold neutral ejected stellar envelope with any substantial mass

⁶ Note that this could be true of SNe II_n-P from low-mass progenitors, as well as for other SNe II_n from more massive stars (see §4.5).

(several M_{\odot}). If there are any surrounding clouds that show evidence for some outward acceleration by radiation pressure from the SN, it is likely that their accelerated mass and momentum are far less than would be expected for a 10^{51} erg blast wave.

4.4 Post-Shock Dust Formation

Recent observations have placed much better constraints on the mass of dust that resides in the dense filaments of the Crab Nebula. Mid-IR observations with *Spitzer* (Temim et al. 2006, 2012) and far-IR observations with *Herschel* (Gomez et al. 2012) yield a surprisingly large mass of 0.1–0.2 M_{\odot} of dust. With a filament gas mass of order 5 M_{\odot} , this would suggest a gas/dust mass ratio of 25–50, significantly higher than in the normal interstellar medium, and indicative of very efficient dust condensation. This indicates that the dust formed from processed stellar ejecta. This dust mass is much higher than that which is deduced from IR measurements of normal SNe II-P, typically of order 10^{-3} M_{\odot} or less (Sugerman et al. 2006; Andrews et al. 2010; Meikle et al. 2007). The IR images of the Crab have sufficient angular resolution to suggest that most of the emitting dust resides in the filaments, and not in a hypothetical envelope outside the Crab. This confirms the indication that dust resides in the filaments themselves, based on the fact that some filaments on the near side of the Crab’s shell are seen in silhouette against the synchrotron continuum (Fesen & Blair 1990).

If the Crab is the result of a Type IIn supernova, then CSM interaction that formed the thin CDS might also have precipitated efficient dust formation. Studies of the Type Ibn event SN 2006jc showed that dust formed efficiently and quickly (~ 50 days after explosion) as the SN ejecta crashed into dense He-rich CSM (Smith et al. 2008a). Mounting evidence from studies of SNe IIn suggest that these compressed post-shock layers may be efficient sites of dust formation in H-rich SNe IIn as well (see Smith et al. 2012, and references therein). The efficient radiative cooling and very high densities in the post-shock zones may lead to much more efficient and rapid dust formation in SNe IIn as compared to normal SNe where the ejecta expand rapidly and the density quickly drops. The drop in luminosity after the plateau of SNe IIn in particular may aid the formation of dust, because the CDS temperature will drop while the density is still very high. Indeed, the very low late-time luminosity and red color of SNe IIn-P like SN 2011ht seem to suggest efficient dust formation (Mauerhan et al. 2013a). Such rapid dust formation in the filaments of the Crab is harder to explain in the standard model of SN 1054 as a normal SN, which lacks such a dense and thin cooling layer.

4.5 The Diverse Progenitors of SNe IIn

Taken together, the Crab Nebula and the sub-class of SNe IIn-P provide strong evidence that a subset of SNe IIn arise from the lowest-mass progenitor stars that can undergo core collapse. These are super-AGB stars in the range 8–10 M_{\odot} that suffer an ecSN rather than an Fe core collapse event.

In that case, the class of SNe IIn must be a fairly heterogeneous collection of explosions, with both very high

mass progenitors and low-mass progenitors. In addition to the low-mass 8–10 M_{\odot} super-AGB stars that may produce SNe IIn-P, some SNe IIn may arise from star systems with even lower initial masses below 8 M_{\odot} ; these are the so-called “hybrid” Type Ia/IIn objects, that seem to result from Type Ia explosions surrounded by dense H-rich CSM, such as SN 2002ic (e.g., Chugai & Yungelson 2004; Silverman et al. 2013; and references therein).

At the other extreme, there are several arguments that SNe IIn are associated with very massive progenitor stars as well. Very luminous SNe IIn like SN 2006gy, SN 2006tf, and others require CSM masses of order 10–20 M_{\odot} in order to power their high luminosity with CSM interaction (Smith et al. 2007, 2008b, 2010a; Smith & McCray 2007; van Marle et al. 2010; Woosley et al. 2007), so their progenitors must have been very massive stars. Even moderately luminous SNe IIn seem to require mass-loss rates that can only be achieved with the eruptive modes of mass loss seen in LBVs (Gal-Yam et al. 2007; Smith et al. 2007, 2008b). There have been 3 clear detections of hypergiant LBV-like progenitors of SNe IIn, including SN 2005gl (Gal-Yam & Leonard 2009; Gal-Yam et al. 2007), SN 1961V (Smith et al. 2011b; Kochanek et al. 2011), and most recently SN 2009ip (Mauerhan et al. 2013b; Smith et al. 2010; Foley et al. 2011). The case of SN 2009ip was particularly interesting, seen as an eruptive LBV that was studied spectroscopically and photometrically before it exploded. Additionally, a luminous blue source is seen at the location of the luminous SN IIn 2010jl, although the SN has not yet faded; this source is either an extremely luminous and massive supergiant or a very young star cluster. Either option would require an initial mass above ~ 30 M_{\odot} (Smith et al. 2011c). Thus, there is strong and direct evidence that very massive LBV-like stars do sometimes explode as SNe IIn. Some lower-luminosity SNe IIn may arise from intermediate masses too, such as 20–40 M_{\odot} red supergiants with extreme winds (see Smith et al. 2009a, 2009b).

Thus, the diverse progenitors of various SNe IIn span a wide range of initial masses. This must be taken into account when interpreting results of the statistical distribution of SNe IIn in galaxies, as compared to other types of SNe (e.g., Anderson et al. 2012; Kelly & Kirshner 2010).

4.6 SN Impostors and ecSNe

The model discussed above casts SN 1054 and the Crab Nebula as the result of a Type IIn-P explosion, similar to SNe 1994W, 2009kn, and 2011ht, where the explosion mechanism was the collapse of a degenerate ONeMg core (i.e. an ecSN) that yields a sub-energetic (10^{50} erg) explosion and low ^{56}Ni mass. A key component of the proposed model is that intense CSM interaction permits the resulting SN to be more luminous than a traditional 10^{51} erg core-collapse SN, but with an order of magnitude lower explosion energy. This reconciles the apparent brightness of SN 1054 with the abundances and low kinetic energy in the Crab.

There are two other classes of explosions that are commonly discussed as possible ecSNe as well. One is the class of sub-luminous SNe II-P that make up the bottom end of the luminosity distribution for SNe II-P (Pastorello et al. 2004, 2009), and which also have directly detected progenitor stars that are near the low-mass end of the distribution

of SN II-P progenitors (Smartt 2009). The low-luminosity SNe II-P show no clear signs of CSM interaction in their spectra, with broader emission lines and P Cygni absorption features that are unlike LBVs or SNe IIn (Smith et al. 2009c). In that case, there is no apparent conflict with the ecSN model suggested here for the Crab, since at least in principle, an ecSN may or may not have dense-enough CSM to raise its luminosity appreciably. With the expected explosion energy and ^{56}Ni yield, the luminosities of the faintest SNe II-P match expectations for ecSN with no significant CSM interaction.

Another class of transients that has been linked to ecSNe by some authors (Thompson et al. 2009; Botticella et al. 2009) is the sub-class of SN impostors whose archetypes are SN 2008S and the 2008 transient in NGC 300 (NGC 300-OT). The motivations for this link are that (1) the progenitors are consistent with short-lived dust-enshrouded stars of relatively low initial mass (Prieto et al. 2008, 2009; Thompson et al. 2009), reminiscent of the super-AGB stars expected as the progenitors of ecSNe, and (2) various factors suggest that the transients are explosive (e.g., Kochanek 2011). With durations of ~ 100 d and peak absolute magnitudes around -14 mag, the total radiated energy of these events is a few 10^{47} erg, or a fraction of only $\sim 10^{-3}$ of the expected explosion energy of an ecSN. This is a factor of 10 lower than the luminosity and radiated energy in the low-luminosity SNe II-P like SN 2005cs.

A potential conflict in this picture is that the spectra of these transients exhibit narrow lines and no significant broad absorption at the times of peak luminosity, similar to the spectra of SNe IIn. This, in turn, suggests that they are dominated by strong CSM interaction. Yet, these SN impostor transients are a factor of ~ 5 less luminous than even the faintest SNe II-P discussed above. CSM interaction can generate a lower luminosity if the dense CSM only occupies a small fraction of the solid angle of the explosion, but in that case the spectrum should also reveal the bare ecSN photosphere (which should show broad lines similar to SN 2005cs), and moreover, the level of dust obscuration around the progenitors seems to require that the dense CSM covers a large fraction of the solid angle. The CSM mass of order $1 M_{\odot}$ around these progenitors (Wesson et al. 2010) and the observed line widths would require that CSM interaction from a 10^{50} erg explosion would either be several times more luminous or would last much longer than 100 days (i.e. as in the 10 yr long Great Eruption of η Carinae, if it was powered by CSM interaction in a 10^{50} erg explosion; Smith 2013), and would convert a larger fraction of the kinetic energy into light. (It is not clear yet if the integrated IR luminosity can make up the difference, but perhaps continued study will answer this.) Because an ecSN that interacts with CSM should be significantly more luminous than the faint SNe II-P, not less luminous, this suggests that SN impostors probably arise from explosive transients of lower energy ($10^{48} - 10^{49}$ ergs). Unless an ecSN can produce an explosion energy this low, there is probably some other physical mechanism for these SN impostors and related transients that is different from the Crab and SNe IIn-P. Discussing these numerous other possibilities is beyond the scope of this paper.

ACKNOWLEDGMENTS

I thank the anonymous referee for helpful comments, and I

thank Rob Fesen for interesting discussions about the observed properties of the Crab Nebula.

REFERENCES

- Arnett, W.D. 1974, *ApJ*, 193, 169
 Anderson, J., et al. 2012, *MNRAS*, 424, 1372
 Andrews, J.E., et al. 2010, *ApJ*, 715, 541
 Arcavi, I., et al. 2012, *ApJ*, 756, L30
 Bietenholz, M.F., Kronberg, P.P., Hogg, D.E., & Wilson, A.S. 1991, *ApJ*, 373, L59
 Blair, W.D., et al. 1997, *ApJS*, 109, 473
 Botticella, M.T., et al. 2009, *MNRAS*, 398, 1041
 Brecher, K., Fesen, R.A., Maran, S.P., & Brandt, J.C. 1983, *Obs.*, 103, 106
 Buta, R.J. 1982, *PASP*, 94, 578
 Chevalier, R.A. 1977, in *Supernovae*, ed. D. Schramm (Dordrecht: Reidel), 53
 Chevalier, R.A., & Irwin, C.M. 2011, *ApJ*, 729, L6
 Chugai, N.N., & Danziger, I. J. 1994, *MNRAS*, 268, 173
 Chugai, N.N., & Yungelson, L.R. 2004, *Astronomy Letters*, 30, 65
 Chugai, N.N., et al. 2004, *MNRAS*, 352, 1213
 Clark, D.H., & Stephenson, R.R. 1977, *The Historical Supernovae* (Oxford: Pergamon)
 Cox, C.I., Gull, S.F., & Green, D.A. 1991, *MNRAS*, 250, 750
 Crotts, A.P.S., et al. 1989, *ApJ*, 347, L61
 Davidson, K., & Fesen, R.A. 1985, *ARA&A*, 23, 119
 Davidson, K., et al. 1982, *ApJ*, 253, 696
 Dessart, L., Hillier, D.J., Li, C., & Woosley, S. 2012, *MNRAS*, 424, 2139
 Duyvendak, J.J.L. 1942, *PASP*, 54, 941
 Elias-Rosa, N., et al. 2009, *ApJ*, 706, 1174
 Falk, S.W., & Arnett, W.D. 1977, *ApJS*, 33, 515
 Fesen, R.A., & Gull, T.R. 1986, *ApJ*, 306, 259
 Fesen, R.A., & Blair, W.D. 1990, *ApJ*, 351, L45
 Fesen, R.A., & Kirshner, R.P. 1982, *ApJ*, 258, 1
 Fesen, R.A., Martin, C.L., & Shull, J.M. 1992, *ApJ*, 399, 599
 Fesen, R.A., Shull, J.M., & Hurford, A.P. 1997, *AJ*, 113, 354
 Frail, D.A., Kassim, N.E., Cornwell, T.J., & Goss, W.M. 1995, *ApJ*, 454, L129
 Foley, R.J., et al. 2011, *ApJ*, 732, 32
 Gal-Yam, A., & Leonard, D.C. 2009, *Nature*, 458, 865
 Gal-Yam, A., et al. 2007, *ApJ*, 656, 372
 Gaensler, B.M. 2001, in *Young Supernova Remnants* (New York: Melville), 295
 Gaensler, B.M., & Slane, P.O. 2006, *ARA&A*, 44, 17
 Glaccum, W., et al. 1982, *BAAS*, 14, 612
 Gomez, H., et al. 2012, *ApJ*, 760, 96
 Graham, J.R., Wright, G.S., & Longmore, A.J. 1990, *ApJ*, 352, 172
 Hachinger, S., et al. 2012, *MNRAS*, 422, 70
 Henry, R.B.C., & MacAlpine, G.M. 1982, *ApJ*, 258, 11
 Hester, J.J. 2008, *ARA&A*, 46, 127
 Hillebrandt, W. 1982, *A&A*, 110, 3
 Kankare, E., et al. 2012, *MNRAS*, 424, 855
 Kelly, P.L., & Kirshner, R.P. 2012, *ApJ*, 759, 107
 Kitaura, F.S., Janka, H.T., & Hillebrandt, W. 2006, *A&A*, 450, 345
 Kochanek, C. 2011, *ApJ*, 741, 37
 Kochanek, C., et al. 2011, *ApJ*, 737, 76
 Kirshner, R.P. 1974, *ApJ*, 194, 323
 Krause, O., et al. 2008a, *Science*, 320, 1195
 Krause, O., et al. 2008b, *Nature*, 456, 617
 Lau, H.H.B., Gil-Pons, P., Doherty, C., & Lattanzio, J. 2012, *A&A*, 542, A1
 Lawrence, et al. 1995, *AJ*, 109, 2635

- Leonard, D. C., et al. 2002, *PASP*, 114, 35
- Li, W., et al. 2011, *MNRAS*, 412, 1441
- Loh, E.D., Baldwin, J.A., & Ferland, G.J. 2010, *ApJ*, 716, L9
- Lundmark, K. 1921, *PASP*, 33, 225
- Lundqvist, P., Fransson, C., & Chevalier, R.A. 1986, *A&A*, 162, L6
- MacAlpine, G.M., McGaugh, S.S., Mazzarella, J.M., & Uomoto, A. 1989, *ApJ*, 342, 364
- MacAlpine, G.M., & Satterfield, T.J. 2008, *AJ*, 136, 2152
- Marsden, P.L., et al. 1984, *ApJ*, 278, L29
- Mayall, N.U., & Oort, J.H. 1942, *PASP*, 54, 95
- Mauche, C.W., & Gorenstein, P. 1989, *ApJ*, 336, 843
- Mauerhan, J.C., Smith, N., Silverman, J.M., Filippenko, A.V., Morgan, A.N., Cenko, S.B., Ganeshalingam, M., Clubb, K.I., Matheson, T. 2013a, *MNRAS*, 431, 2599
- Mauerhan, J.C., et al. 2013b, *MNRAS*, 430, 1801
- Meikle, W.P.S., et al. 2007, *ApJ*, 665, 608
- Miller, J.S. 1973, *ApJ*, 180, L83
- Minkowski, R. 1970, *PASP*, 82, 470
- Minkowski, R. 1971, *IAUS*, 46, 241
- Miyajo, S., Nomoto, K., Yokoi, K., & Sugimoto, S. 1980, *PASJ*, 32, 303
- Morse, J.A., Smith, N., Blair, W.P., Kirshner, R.P., Winkler, P.F., & Hughes, J.P. 2006, *ApJ*, 644, 188
- Nomoto, K., Sugimoto, D., Sparks, W.M., Fesen, R.A., Gull, T.R., & Miyaji, S. 1982, *Nature*, 299, 803
- Nomoto, K. 1987, *ApJ*, 277, 791
- Nugent, R.L. 1998, *PASP*, 110, 831
- Ott, C.D., Burrows, A., Thompson, T.A., Livne, E., & Walder, R. 2006, *ApJS*, 164, 130
- Pastorello, A., et al. 2007, *Nature*, 474, 892
- Pastorello, A., et al. 2009, *MNRAS*, 394, 2266
- Pequignot, D., & Dennefeld, M. 1983, *A&A*, 120, 249
- Poelarends, A.J.T., Herwig, F., Langer, N., & Heger, A. 2008, *ApJ*, 675, 614
- Predehl, P., & Schmitt, J.H.M.M. 1995, *A&A*, 293, 889
- Prieto, J.L., et al. 2008, *ApJ*, 681, L9
- Prieto, J.L., et al. 2009, *ApJ*, 705, 1425
- Rest, A., et al. 2005, *Nature*, 438, 1132
- Rest, A., et al. 2008a, *ApJ*, 680, 1137
- Rest, A., et al. 2008b, *ApJL*, 681, L81
- Rest, A., et al. 2011a, *ApJ*, 732, 3
- Rest, A., et al. 2011b, *ApJ*, 732, 2
- Rest, A., et al. 2012, *Nature*, 482, 375
- Reynolds, S. 1985, in *The Crab Nebula and Related Supernova Remnants* (Cambridge: Cambridge University Press), 173
- Rudie, G.C., Fesen, R.A., & Yamada, T. 2007, *MNRAS*, 384, 1200
- Sankrit, R., et al. 1998, *ApJ*, 504, 344
- Satterfield, T.J., Katz, A.M., Sibley, A.R., MacAlpine, G.M., & Uomoto, A. 2012, *AJ*, 144, 27
- Seward, F.D., Harnden, D., & Helfand, D. 1984 *ApJ*, 287, L19
- Seward, F.D., Gorenstein, P., & Smith, R.K. 2006, *ApJ*, 636, 873
- Silverman, J., et al. 2013, preprint (arXiv:1304.0763)
- Smartt, S.J. 2009, *ARA&A*, 47, 63
- Smith N. 2003, *MNRAS*, 346, 885
- Smith N. 2013, *MNRAS*, 429, 2366
- Smith, N., & McCray, R. 2007, *ApJ*, 671, L17
- Smith, N., et al. 2007, *ApJ*, 666, 1116
- Smith, N., Foley, R.J., & Filippenko, A.V. 2008a, *ApJ*, 680, 568
- Smith, N., et al. 2008b, *ApJ*, 686, 467
- Smith, N., Hinkle, K., & Ryde, N. 2009a, *AJ*, 137, 3558
- Smith, N., et al. 2009b, *ApJ*, 695, 1334
- Smith, N., et al. 2009c, *ApJ*, 697, L49
- Smith, N., Chornock, R., Silverman, J.M., Filippenko, A.V., & Foley, R.J. 2010a, *ApJ*, 709, 856
- Smith, N., et al. 2010b, *AJ*, 139, 1451
- Smith, N., Li, W., Filippenko, A.V., & Chornock, R. 2011a, *MNRAS*, 412, 1522
- Smith, N., et al. 2011b, *MNRAS*, 415, 773
- Smith, N., et al. 2011c, *ApJ*, 732, 63
- Smith, N., et al. 2012, *AJ*, 143, 17
- Sollerman, J., et al. 2000, *ApJ*, 537, 861
- Sollerman, J., Kozma, C., & Lundqvist, P. 2001, *A&A*, 366, 197
- Sugerman, B.E.K., et al. 2005, *ApJS*, 159, 60
- Sugerman, B.E.K., et al. 2006, *Science*, 313, 196
- Sugerman, B.E.K., Andrews, J.E., Barlow, M.J., et al. 2012, *ApJ*, 749, 170
- Temim, T., et al. 2006, *ApJ*, 132, 1610
- Temim, T., et al. 2012, *ApJ*, 753, 72
- Temim, T., & Dwek, E. 2013, preprint (arXiv:1302.5452)
- Thompson, T.A., et al. 2009, *ApJ*, 705, 1364
- Trimble, V. 1968, *AJ*, 73, 535
- Trimble, V. 1973, *PASP*, 85, 579
- Uomoto, A., & MacAlpine, G.M. 1987, *AJ*, 93, 1151
- van Marle, A.J., Smith, N., Owocki, S.P., & van Veelen, B. 2010, *MNRAS*, 407, 2305
- Wanajo, S., Nomoto, K., Janka, H.T., Kitaura, F.S., & Muller, B. 2009, *ApJ*, 695, 208
- Weaver T.A., & Woosley, S.E. 1979, *BAAS*, 11, 724
- Weiler, K.W. 1983, *Observatory*, 103, 85
- Weiler, K.W., & Seielstad, G.A. 1971, *ApJ*, 163, 455
- Wesson, R., et al. 201, *MNRAS*, 403, 474
- Woltjer, L. 1958, *Bull. Astron. Inst. Neth.*, 14, 39
- Wood, P.R., & Faulkner, D.J. 1986, *ApJ*, 307, 659
- Woosley et al. 2007, *Nature*, 450, 390
- Wyckoff, S., & Murray, C.A. 1977, *MNRAS*, 180, 717